Experimental assessment of sound quality metrics for takeoff and landing aircraft

Vieira, Ana; Snellen, Mirjam; Simons, Dick G.

DOI
10.2514/1.J059633

Publication date
2021

Document Version
Final published version

Published in
AIAA Journal

AIAA JOURNAL
Vol. 59, No. 1, January 2021

Experimental Assessment of Sound Quality Metrics for Takeoff and Landing Aircraft

Ana Vieira,* Mirjam Snellen,† and Dick G. Simons‡
Delft University of Technology, 2629 HS Delft, The Netherlands

https://doi.org/10.2514/1.J059633

The reduction of aircraft noise over the past decades has generated a growing awareness that the characteristics of a signal can be equally or more important to annoyance than the sound pressure level. Sound can be perceived as more annoying, depending on the frequency content or tonal components. The sound quality metrics loudness, roughness, sharpness, and tonality are important tools to characterize sound. Flyover measurements of landing and takeoff aircraft are investigated in terms of sound quality metrics. The experimental dataset includes 141 measurements of 14 landing aircraft types and 160 measurements of 12 takeoff aircraft types. The sound quality metrics are compared for different aircraft types, and their variability within the same aircraft is investigated. Possible correlations of the sound quality metrics with the airframe, engines, and aircraft operational conditions are investigated. This analysis provides empirical expressions that show a good agreement with experimental data for loudness, sharpness, and roughness for takeoff aircraft. For landing aircraft, empirical expressions could only be obtained for loudness and tonality.

Nomenclature

A_{Ek}	=	amplitude of the secondary neural excitation, dB
c	=	calibration function for tonality
E_{Gr}	=	masking intensity of noise in critical bands surrounding the tone, dB
E_{HS}	=	intensity at the threshold of hearing, dB
f_{mod}	=	modulation frequency, Hz
g	=	weighting function for sharpness
H	=	absolute altitude, m
K	=	tonality unit, t.u.
L_E	=	excitation level per critical band, dB
L_i	=	sound pressure level of a tonal component, dB
L_{TQ}	=	excitation level at the threshold in quiet conditions, dB
N	=	loudness, sone
N_1	=	rotational speed of the fan, %
N_s	=	specific loudness, sone/Bark
N'	=	unmasked specific loudness, sone
R	=	roughness, asper
S	=	sharpness, acum
v_{Gr}	=	total ground speed, m/s
w_{Gr}	=	broadband noise weighting function
w_T	=	total weighting function
w_1	=	bandwidth weighting function
w_2	=	frequency weighting function
w_3	=	prominence weighting function
z	=	critical band rate, Bark
ΔL_m	=	modulation depth, dB
ϕ	=	diameter, m

Presented as Paper 2019-2512 at the 25th AIAA/CEAS Aeroacoustics Conference, Delft, The Netherlands, January 20–23, 2019; received 2 April 2020; revision received 23 July 2020; accepted for publication 17 September 2020; published online 5 November 2020.

*Ph.D. Candidate, Aircraft Noise and Climate Effects Section, Faculty of Aerospace Engineering; a.e.alvesvieira@tudelft.nl.

†Full Professor, Aircraft Noise and Climate Effects Section, Faculty of Aerospace Engineering; m.snellen@tudelft.nl.

‡Full Professor, Aircraft Noise and Climate Effects Section, Faculty of Aerospace Engineering; d.g.simons@tudelft.nl.

I. Introduction

AIRCRAFT noise is associated with serious health problems, such as heart diseases and stress, in communities near airports [1]. Traditional noise metrics such as the A-weighted maximum sound pressure level $L_{A,\max}$, the sound exposure level (SEL), and the effective perceived noise level (EPNL) are used to assess the noise perceived on the ground. However, these metrics do not provide information about the characteristics of a sound, and two sound signals with equal noise levels are not necessarily perceived as equivalent by the receiver [2–4].

Sound quality metrics (SQMs) are associated with different noise characteristics, such as the frequency content (high or low frequency), the prominence of tones, and the fast or slow loudness fluctuations. The five SQMs loudness, roughness, sharpness, tonality, and fluctuation strength provide a detailed characterization of a sound; and they can be combined toward an overarching psychoacoustic metric. These metrics then provide a single value similar to the EPNL and $L_{A,\max}$, allowing us to compare the annoyance of different sounds. Recent work considered the psychoacoustic metrics as a more accurate method to determine the annoyance perceived by the human ear than EPNL [5].

The sound quality metrics can be associated with different noise sources during a flyover, e.g., tonality is associated with fan noise for landing and roughness with buzz-saw noise for takeoff. The aircraft design and flight trajectory can be driven by the SQMs with the objective of lowering annoyance in areas near airports [6,7], which is a process widely implemented using traditional metrics: more commonly, the EPNL and SEL [8,9].

This contribution intends to understand the SQMs for takeoff and landing aircraft using experimental data. Approximately 300 landing and takeoff flyover measurements are analyzed for 17 different aircraft types. The average value and the variability of loudness, roughness, sharpness, and tonality are investigated for each aircraft type: both for landing and takeoff. Preliminary research indicated the existence of correlations between the SQMs and the aircraft design during landing [10]. Correlations between the SQMs and the aircraft airframe, engines settings, and operating conditions are further investigated in this work. This analysis aims to assess whether the SQMs can be associated to the aircraft design and if it is possible to find empirical expressions that relate them. Such empirical expressions would allow the design of less annoying aircraft in the perception of the residents, without necessarily implying an overall reduction of many decibels.

II. Sound Quality Metrics

The four sound quality metrics used in this work (loudness, sharpness, roughness, and tonality) are briefly described in this section, and the methods used to calculate them are presented.

Aircraft noise is not steady in time, and the SQMs change during the flyover. Therefore, the values of loudness N_5, tonality K_5, sharpness S_5, and roughness R_5 in this work refer to the values exceeded 5% of the time.

A. Loudness

Loudness is the subjective perception of the magnitude of a sound, and it is dependent on its frequency, intensity, and duration. Loudness has been standardized in the International Organization for Standardization's STD ISO 532-1 [11,12], and it is expressed in phon (when in logarithmic scale) or sone (in linear scale).

The specific loudness N_s, which is the loudness of the 24 critical frequency bands z, is calculated using

$$N_s(z) = 0.0635\left[10^{0.025L_{\mathrm{TQ}}(z)}\right] \times \left[\left(0.75 + 0.25\left\{10^{0.1[L_E(z)-L_{\mathrm{TQ}}(z)]}\right\}\right)^{0.25} - 1\right] \quad (1)$$

where L_E and L_{TQ} are the excitation level and the threshold in quiet conditions, respectively. These two parameters were calculated following the methodology of Terhardt [13]. The critical bands concept was introduced by Harvey Fletcher [14] and it is related to the neural activity of the human ear.

The values of specific loudness are determined in each of the 24 critical bands, and it is checked whether they are masked by a sound concentrated in an adjacent critical band. The results are values of unmasked specific loudness in each critical band N', which are used to determine the total loudness N, calculating the area below the curve of N' over the critical bands:

$$N = \int_0^{24} N'(z)\,\mathrm{d}z \quad (2)$$

B. Sharpness

Sharpness quantifies the high-frequency content of a sound: a sound perceived as sharper has more high-frequency content. This work uses the method of von Bismarck [15] to determine sharpness S, which is given by

$$S = 0.11\,\frac{\int_0^{24} N'(z)g(z)z\,\mathrm{d}z}{N} \quad (3)$$

Here, $g(z)$ is a weighting function given by

$$g(z) = \begin{cases} 1 & 0 < z \le 16 \\ 0.066e^{0.171z} & 16 < z \le 24 \end{cases} \quad (4)$$

This weighting function causes the value of sharpness to be higher for signals with more content in the higher critical bands.

C. Tonality

The tonal content of a sound is an important characteristic in aircraft noise, and traditional metrics such as the tone corrected perceived noise level (PNL) and the effective perceived noise level (EPNL) include tone penalties. In this work, the sound quality metric tonality is calculated using Aures's method [16].

In this method, all the tones are identified and checked if *aurally relevant*. This is done by calculating the sound pressure level (SPL) excess ΔL_i using the method of Terhardt et al. [17]. The value of ΔL_i is given by

$$\Delta L_i = L_i - 10\log_{10}\left\{\left[\sum_{k\neq i}^{n} A_{\mathrm{Ek}}(f_i)\right]^2 + E_{\mathrm{Gr}}(f_i) + E_{\mathrm{HS}}(f_i)\right\} \quad (5)$$

If the value of ΔL_i is larger than zero, the tone is considered aurally relevant. In Eq. (5), L_i is the SPL of the tonal component i and the term A_{Ek} is the amplitude of the secondary neural excitation of frequency f_i due to the k^{th} tone. The sum of A_{Ek} takes into account the mutual masking effect of all tonal components. The term E_{HS} is the intensity at the threshold of hearing, and E_{Gr} is the masking intensity of the broadband noise surrounding the selected tones. Expressions for A_{Ek}, E_{HS}, and E_{Gr} can be found in Ref. [17].

The values of ΔL_i aurally relevant are then used to calculate weighting functions of factors that contribute to tonality: the prominence of the tones w_3, the frequency w_2, and the bandwidth w_1:

$$w_1(\Delta z_i) = \frac{0.13}{0.13 + \Delta z_i} \quad (6)$$

$$w_2(f_i) = \left[\sqrt{1 + 0.2\left(\frac{f_i}{700} + \frac{700}{f_i}\right)^2}\right]^{-0.29} \quad (7)$$

$$w_3(\Delta L_i) = (1 - e^{-(\Delta L_i/15)})^{0.29} \quad (8)$$

These three weighting functions are combined into a total weighting function:

$$w_T = \sqrt{\sum_{i=1}^{n} [w_1'(\Delta z_i)w_2'(f_i)w_3'(\Delta L_i)]^2} \quad (9)$$

where $w_l' = w_l^{1/0.29}$ for $l = 1, 2, 3$.

Finally, the value of tonality is given by

$$K = cw_T^{0.29}w_{\mathrm{Gr}}^{0.79} \quad (10)$$

where c is a calibration constant equal to 1.09. The term w_{Gr} introduces the effect of broadband noise, and it is calculated using

$$w_{\mathrm{Gr}} = 1 - \frac{N_{\mathrm{Gr}}}{N} \quad (11)$$

where N_{Gr} is the loudness of the sound without the tones.

D. Roughness

Roughness assesses fast loudness fluctuations (between 50 to 90 Hz). One of the first methods to estimate roughness was developed by Zwicker and Fastl [18]. It was found that two characteristics of the ear influence the roughness perception: the frequency selectivity of the hearing system at low frequencies, and the limited temporal resolution at high frequencies. The model of roughness proposed by Zwicker and Fastl takes into account temporal masking. Figure 1 shows the relation between a masker and its temporal masking pattern (in a solid black line).

In Fig. 1, f_{mod} is the modulation frequency, which is the interval between two consecutive peaks of the masker envelope; and $\Delta L_m(z)$ is the modulation depth of the specific loudness at the critical band z.

According to the Zwicker and Fastl model, roughness is given by

$$R = 0.3f_{\mathrm{mod}}\int_0^{24} \Delta L_m(z)\,\mathrm{d}z \quad (12)$$

Here, z is the critical band rate, as defined before, in the loudness and sharpness metrics.

The calculation of the modulation depth can be challenging for complex signals, and its value can change for different critical bands. A more practical approach is deriving roughness from the specific loudness pattern: an approach used by Aures [19] and further improved by Daniel and Weber [20]. The latter method was used to calculate roughness in this work.

III. Experimental Setup

The flyover measurements were recorded at Amsterdam Airport Schiphol on days with similar weather conditions. The meteorological data were provided by the Royal Netherlands Meteorological Institute. The measurement system, shown in Fig. 2, is an acoustic array of

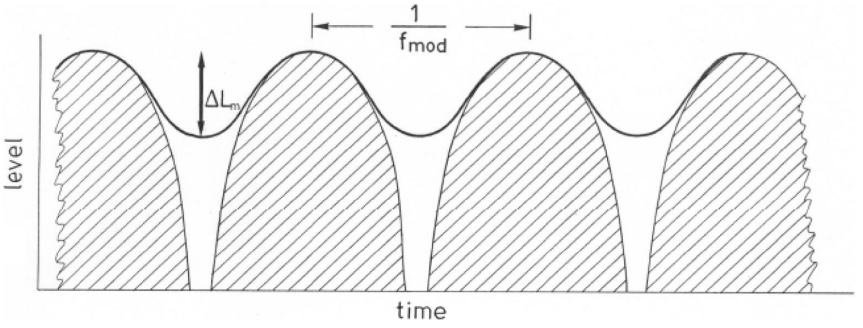

Fig. 1 Scheme of temporal masking used by Zwicker and Fastl [18].

Fig. 2 Acoustic camera used to record the flyovers at Amsterdam Airport Schiphol.

64 microphones distributed in an Underbrink spiral configuration [21]. These microphones can be used collectively to localize noise sources through beamforming techniques. The array has the dimensions of 4×4 m, and its structure is covered with acoustic absorbing foam to minimize sound reflections. The foam selected was Flamex GU with 15 mm thickness due to its high absorption coefficient. All the microphones were covered with wind shields and were calibrated with a piston phone.

The microphone (PUI Audio 665-POM-2735P-R [22]) signals were sampled at 50 kHz. Also, an optical camera was used (Datavision UI-1220LE with a Kowa LM4NCL lens), which had a frame rate of 30 Hz. The camera is placed at the center of the array to determine the overhead time and to localize the main acoustic noise sources using beamforming. Images from the camera can be overlapped with beamforming plots, allowing the localization of the noise sources on the aircraft.

The type of aircraft as well as its height and velocity were determined using an automatic dependent surveillance-broadcast (ADS-B) receiver. Since not all aircraft have an ADS-B transponder, the aircraft type was also verified with online flight trackers, and consecutive frames of the optical camera were used to estimate the height and velocity.

The acoustic array was positioned at an extension of Runway 18C of the airport, represented in Fig. 3. This location was chosen because of its proximity to the runway (670 m) and considerable distance from main roads, and so car traffic would not contaminate the results.

IV. Experimental Results

This section analyzes the landing and takeoff flyover measurements recorded at Amsterdam Airport Schiphol in terms of SQMs and their variability within the same aircraft type. The SQMs differ for distinct aircraft designs, but also for different operating conditions. Consequently, these metrics have different behaviors for landing and takeoff.

It is explored whether the sound quality metrics correspond to the theoretical expected behavior during landing and takeoff for the different aircraft types and if correlations between the SQMs and the aircraft design and operational conditions can be found.

Fig. 3 Runways of Amsterdam Airport Schiphol: the runway selected for the measurements (in a red circle), and the approximate measuring location (represented by a black cross).

A. Assessment of Sound Quality Metrics for Landing and Takeoff Flyovers

The experimental campaign at Amsterdam Airport Schiphol resulted in a total of 141 flyover measurements of 14 landing aircraft types, as well as 160 measurements of 12 takeoff aircraft types. Table 1 shows the different aircraft types, ordered by their value of maximum takeoff weight (MTOW), and the corresponding number of landing and takeoff measurements.

The Boeing 737-800 (B737-800), Airbus A320 (A320), and Embraer 190 and 195 models (ERJ-190 and ERJ-195, respectively) correspond to the highest number of measurements for landing and takeoff.

Some aircraft types are not available for both takeoff and landing, for example, the Fokker 70 (F70) and the Boeing 787 (B787). This dataset contains aircraft with very different characteristics: small aircraft with capacity for less than 100 passengers, such as the Bombardier CRJ-900 and the ERJ-190; medium-range aircraft (the B737 and the A320 series); and long-range aircraft (B777 series). The dataset only contains turbofan-propelled aircraft; all of them are twin engine, with the exception of the AVRO-RJ85, which has four engines. Three of the aircraft have rear-mounted engines, the F70, the CRJ-900 and the CRJ-700, and therefore engine noise is partially shielded by the wings and fuselage [23,24].

The flight trajectories during landing are more regular than the ones of takeoff because all aircraft follow the instrument landing system approach. The flight trajectory and aircraft operating conditions

Table 1 Landing and takeoff flyovers recorded in Amsterdam Airport Schiphol

Aircraft	Number of landings	Number of takeoffs
CRJ-700	0	5
CRJ-900	2	0
ERJ-175	14	22
F70	7	0
AVRO-RJ85	3	0
ERJ-190	22	15
ERJ-195	0	4
B737-700	15	15
A319	3	8
A320	13	19
B737-800	41	53
B737-900	4	4
A321	3	5
A330-200	0	5
B787	6	0
B777-200	5	0
B777-300	3	5
Total	141	160

influence the SQMs measured on ground and should be taken into account in this analysis. Figures 4–6 show the variability of the absolute altitude H, the total ground speed V_{Gr}, and the speed of the low-pressure shaft of the fan N_1 (obtained from the spectrograms), estimated for all the aircraft, during landing and takeoff. The aircraft types are presented in ascending order of their value of MTOW.

The distance between the aircraft and the microphone array is approximately 10 times larger for the takeoff measurements than for the landing. This difference has to be taken into consideration when analyzing the SQMs because atmospheric attenuation is distance dependent. The variability of altitude within aircraft type is also higher for the takeoff measurements, which was expected, due to the more irregular flight trajectories compared with landing procedures.

The average ground speed measured for landing flyovers varies between 60 and 80 m/s, whereas for takeoff, the values are between 70 and 90 m/s. Values for N_1 were obtained from the spectrograms, i.e., derived from the acoustic measurements. The variability of N_1 is very significant for some aircraft during landing (e.g., the B787 and the A321), with most aircraft presenting an average value between 50 and 65%. The values of N_1 for takeoff flyovers show less variability

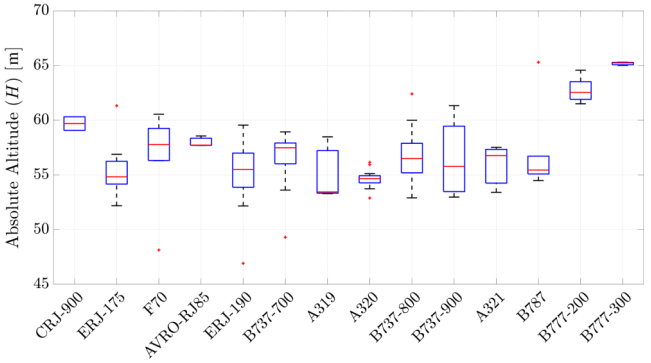

a) Landing

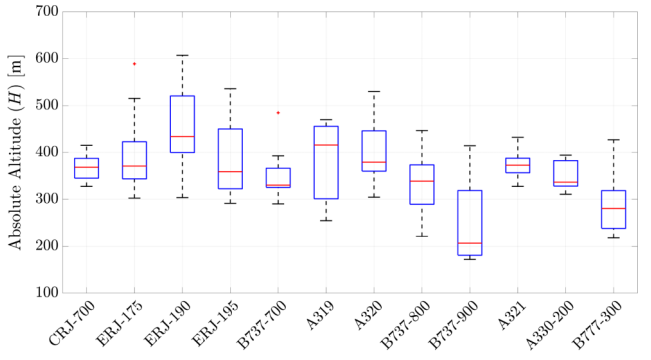

b) Takeoff

Fig. 4 Altitude for landing and takeoff flyovers.

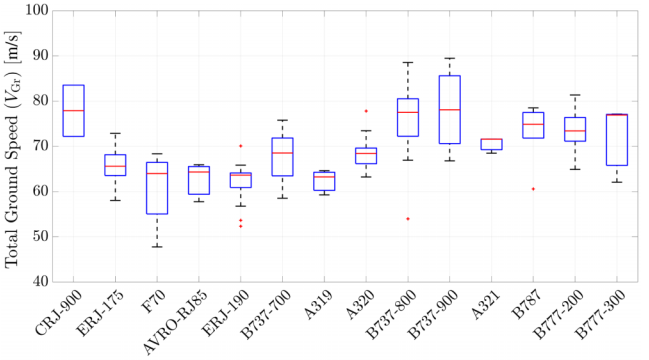

a) Landing

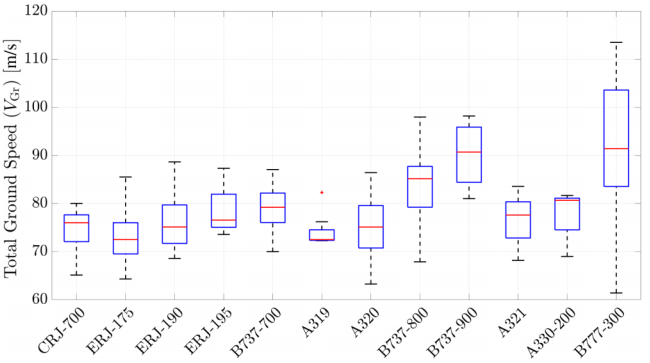

b) Takeoff

Fig. 5 Total ground speed for landing and takeoff flyovers.

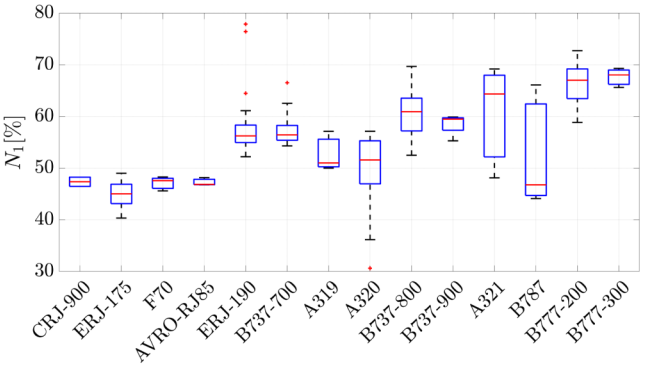

a) Landing

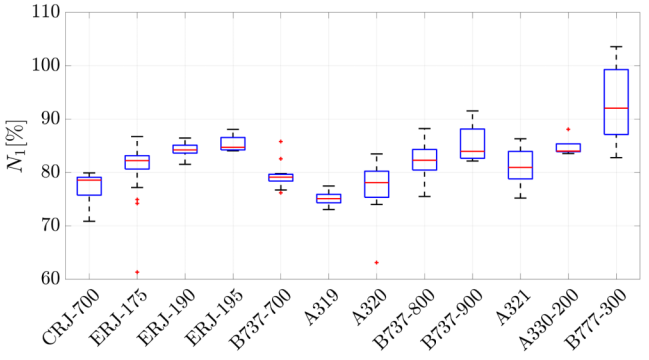

b) Takeoff

Fig. 6 N_1 for landing and takeoff flyovers.

within the same aircraft type than landing, with the exception of a few flyovers that show extremely low values of N_1 for takeoff.

Similar plots are presented for the SQMs in Figs. 7–10. Figure 7 shows that loudness increases with the dimension of the aircraft, as expected, as larger surfaces generate higher levels of airframe noise but also require more powerful engines, and consequently generate higher levels of engine noise as well. The variability of loudness is small for landing aircraft but very significant during takeoff. During landing, fan noise and airframe noise (especially landing gear noise and flap noise) have approximately the same importance. The airframe noise contribution is roughly constant because it depends on the aircraft structure (e.g., landing gear [25] and high lift devices

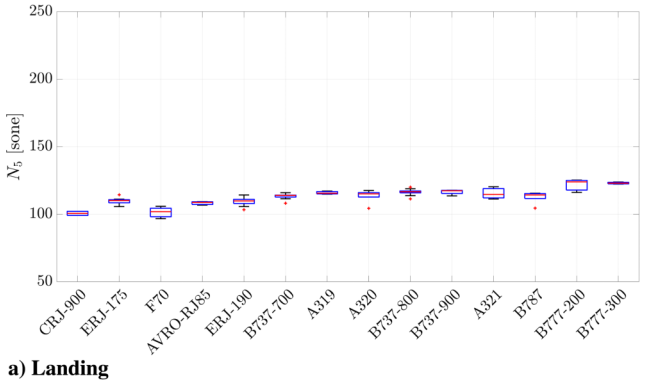

a) Landing

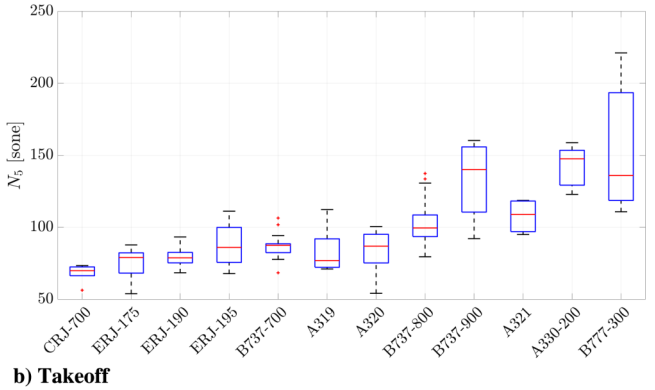

b) Takeoff

Fig. 7 Loudness for landing and takeoff flyovers.

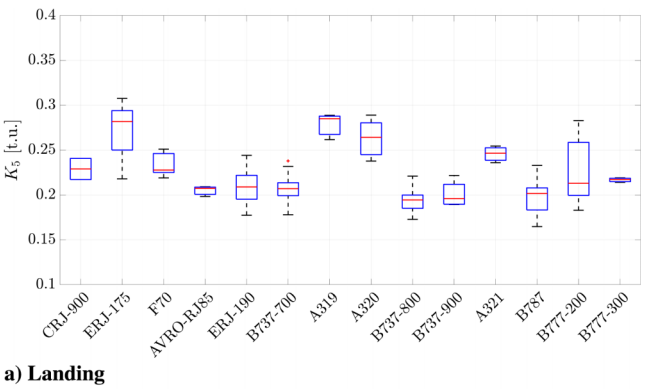

a) Landing

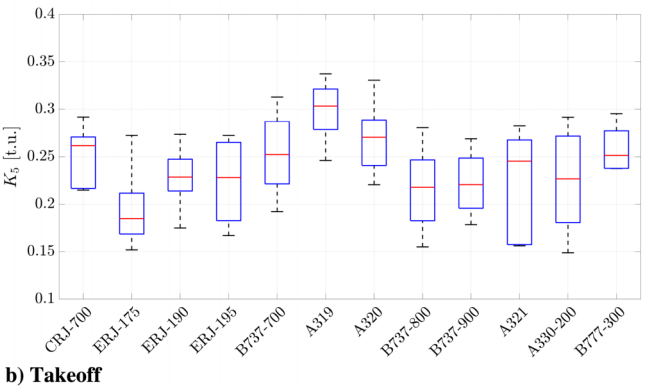

b) Takeoff

Fig. 8 Tonality for landing and takeoff flyovers.

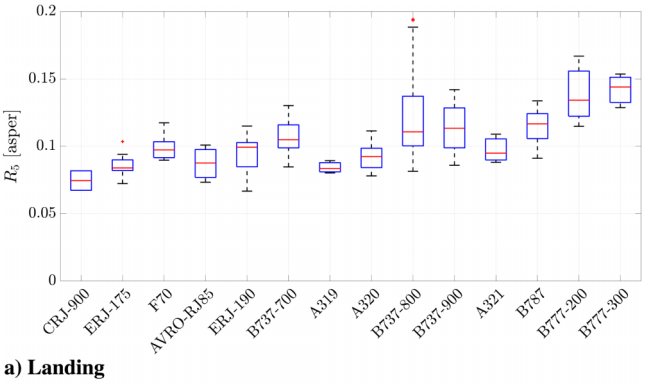

a) Landing

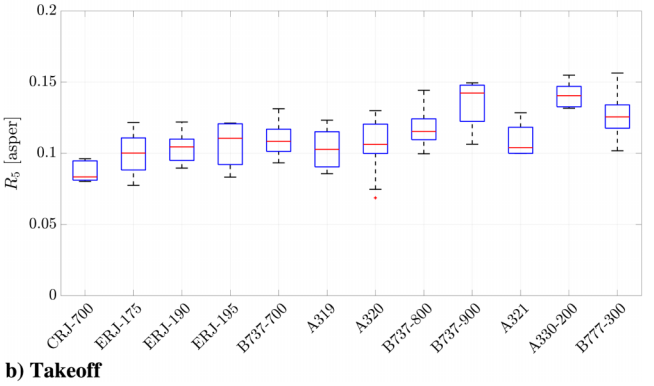

b) Takeoff

Fig. 9 Roughness for landing and takeoff flyovers.

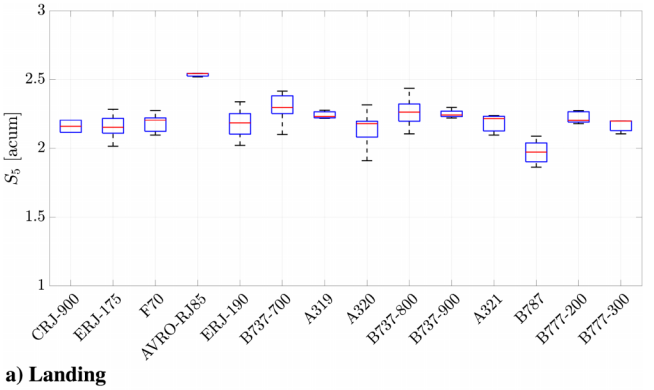

a) Landing

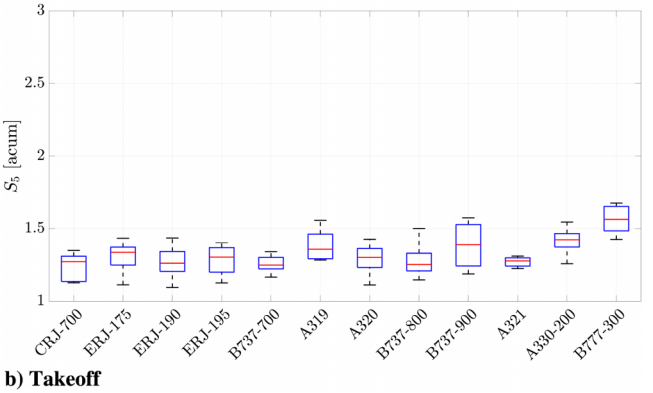

b) Takeoff

Fig. 10 Sharpness for landing and takeoff flyovers.

[26]), flap deflection, and the aircraft velocity. In addition, the landing measurements were recorded with the aircraft at very similar altitudes. Both explain the low variability of loudness for landing aircraft. The aircraft with the lowest values of loudness are the F70, the CRJ-900, and the CRJ-700. These aircraft are equipped with rear-mounted engines, and therefore engine noise is partially shielded by the airframe.

For the takeoff measurements, however, the engines are the most important noise source; and a variation of the engine settings is reflected in the total noise. Also, the trajectories for takeoff are more irregular; and these two factors result in a high variability of loudness. The average values of loudness are higher for landing than for takeoff, which is contrary to what one would expect. However, the aircraft are at a higher altitude for the takeoff measurements, and therefore perceived as less loud.

The tonality plots of Fig. 8 show approximately the same average values for landing and takeoff. The A319 and A320 stand out for their high values of tonality compared to aircraft of similar size: for instance, the B737-700 and 800. Prominent tones were expected for landing due to the high contribution of fan noise, which generates strong tones at frequencies between 1000 and 2000 Hz. During takeoff, the engines are at the maximum performance and the blade passing frequency (BPF) is higher, as well as its harmonics, which increases tonality. However, tones can be masked by the low-frequency noise generated by the jet. In addition, tones at high frequency are attenuated more strongly by the atmosphere. Modern engines have higher values of bypass ratio (BPR) to decrease the velocity of the jet, and consequently jet noise. The BPR of the engines of the A319 and A320 is higher than six. All the other aircraft recorded during takeoff are equipped with engines with lower BPRs, between 5 and 5.5 (except the B777-300, which is a long-range aircraft), which justifies the high value of tonality of the A319 and A320. The similar values of tonality for landing and takeoff will be later investigated using spectrograms and the signal power spectral density.

Also the values of roughness, shown in Fig. 9, are similar for takeoff and landing. Takeoff aircraft are expected to generate rougher sounds than landing because of buzz-saw noise. Buzz-saw noise is generated when the fan tips operate at supersonic speed, generating weak shock waves spiraling upstream against the mean flow [27,28]. This behavior generates periodic noise, denominated as buzz-saw noise (BSN) tones, which decreases with frequency. Irregularities in the mean flow and spacing of shock waves make this phenomenon difficult to predict.

During landing, low-frequency noise is associated with airframe noise, which is more dominant during this flight phase than takeoff. The increase of this metric with the MTOW values also indicates a relation with the dimensions of the aircraft. The similarity in roughness during takeoff and landing will be explored further ahead in this research work.

Finally, Fig. 10 shows the values of sharpness and its variability for each aircraft type. The values are noticeable higher for landing. The sharpness values for takeoff are low because jet noise masks the harmonics of fan noise. In addition, the first harmonics of fan noise, which are of higher frequency for takeoff than for landing, are strongly attenuated by the atmosphere. The AVRO-RJ85 shows the highest value of sharpness because it is the only four-engine aircraft in the dataset.

Figure 11 shows the spectrogram of an A320 takeoff flyover and the spectrum at overhead time. This A320 aircraft is equipped with CFM56-5A engines with 36 fan blades. The BPF of the fan and its second harmonic are clearly visible in the spectrum at 2650 and 5300 Hz, respectively. Other peaks appear at lower frequencies (the buzz-saw noise tones) spaced at 74 Hz. Only the most prominent BSN tones are identified in Fig. 11 for easy reading.

The spectrogram and the spectrum at the overhead time for an A320 landing flyover is shown in Fig. 12. The BPF value is lower than in takeoff due to the lower rotational velocity of the fan. The first four harmonics of the fan are very clear and with a high SPL value. The spectrum of Fig. 12b has more high-frequency content than the takeoff spectrum of Fig. 11b. The aircraft altitude is lower at landing; therefore, the noise is less attenuated by the atmosphere. This explains the higher values of sharpness found for landing, as mentioned before.

The roughness for landing and takeoff measurements is similar; in this case, we can see that the low-frequency content has approximately the same SPL value for landing and takeoff. Even though takeoff presents buzz-saw noise, the BSN tones are not very prominent; during landing, the strong presence of low-frequency airframe noise contributes to roughness, which results in similar values of this sound quality metric for these two phases of flight.

The value of tonality is also identical for the landing and takeoff measurements of the A320. Even though more harmonics of the fan are present during landing, takeoff exhibits BSN tones and the two first harmonics of the fan as well, which balance the values of tonality for the two flight phases.

The aircraft altitude has a direct effect on sharpness and tonality because the high-frequency content is strongly attenuated by the atmosphere. High-frequency noise is more relevant during takeoff because of the higher value of N_1. However, the rate of climb for takeoff is higher than the glide slope for landing, which means that for areas outside the airport, aircraft fly at higher altitudes for takeoff. Consequently, the high-frequency content is strongly attenuated during takeoff.

The analysis of this section shows that the SQMs depend on the aircraft design but also on the operating conditions of the aircraft; and neglecting the latter leads to erroneous assumptions.

B. Correlation of the SQMs with the Aircraft Design

This section investigates correlations between the SQMs and characteristics of the aircraft design and the engine. Such correlations are determined separately for landing and takeoff, and using the

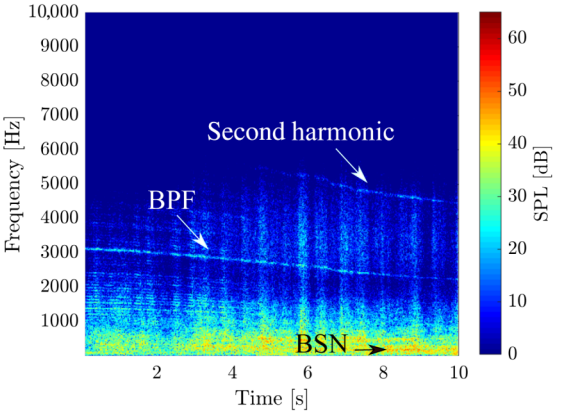

a) Spectrogram

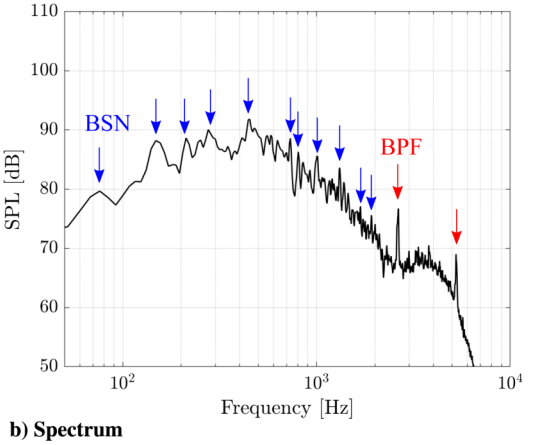

b) Spectrum

Fig. 11 Spectrogram and spectrum at the overhead time for a takeoff measurement of an A320: $N_5 = 76$ sone, $S_5 = 1.18$ acum, $K_5 = 0.32$ t.u., and $R_5 = 0.10$ asper.

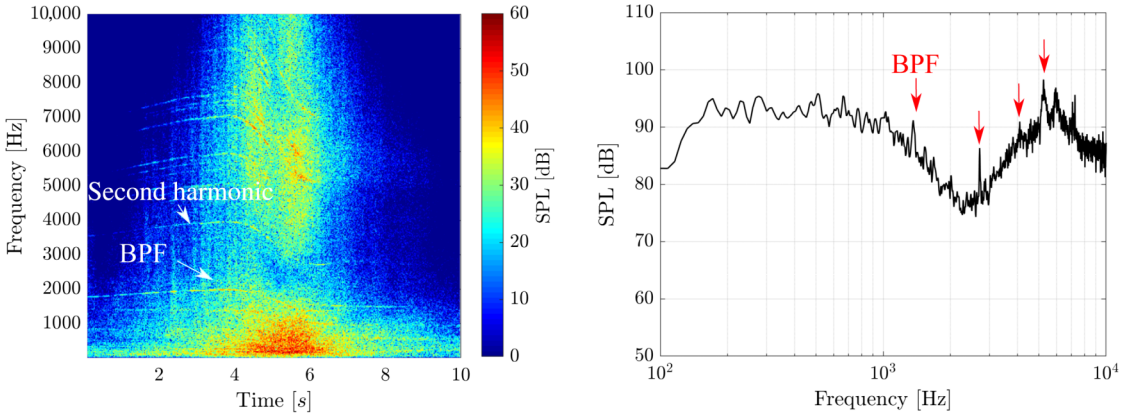

a) Spectrogram b) Spectrum

Fig. 12 Spectrogram and spectrum at the overhead time for a landing measurement of an A320: $N_5 = 115.8$ sone, $S_5 = 2.20$ acum, $K_5 = 0.27$ t.u., and $R_5 = 0.09$ asper.

average values of the SQMs of each aircraft type. The best correlations are employed to find empirical expressions for the SQMs that could be used for an aircraft at the design phase.

A variety of aircraft characteristics was considered in this study. The airframe characteristics considered were the wingspan, the total height, the length of the aircraft, the cabin width, the MTOW, the maximum landing weight (MLW), the ratio flap/span of the wing, and the diameter and number of wheels in the main and nose landing gear. The engine parameters examined were the number of fan blades, the BPR, the diameter of the fan, the length of the nacelle, the maximum takeoff thrust, and the thrust-specific fuel consumption.

For takeoff, loudness showed a good correlation with the dimensions of the aircraft, e.g., the wing span and MTOW. Also, characteristics related with the size of the engine, such as the fan diameter and maximum takeoff thrust, showed a significant correlation. This was expected because the loudness of an aircraft is directly related with its dimension, as seen in the previous section. Roughness also showed dependence on the aircraft dimensions, the diameter of the fan, and the maximum takeoff thrust. Sharpness, however, has high correlations with engine parameters such as the BPR, the diameter of the fan and the length of the nacelle, which is expected because high-frequency noise is mostly generated by the engine. No correlations were observed for tonality during takeoff.

For landing, loudness showed the same correlations as for takeoff, but dependence on the landing gear configuration was also observed. Roughness presented high correlations with many parameters in common with takeoff. Sharpness did not present any correlations. The same was verified for tonality, which was not expected due to the tonal components from the fan.

The aircraft characteristics showing higher values of correlation with the experimental SQMs values were combined in linear equations, and the coefficients were found using multiple linear regression. These equations consider the average values of the SQMs for each aircraft type, and no operational conditions were accounted for. Table 2 shows the correlation coefficients squared R^2 and corresponding p-values obtained for the correlations of the obtained linear expressions with experimental data for each SQM for takeoff. Table 3 shows the results obtained for the landing aircraft. The aircraft parameters used in the linear expressions are also presented. At this point, the coefficients are not presented because these expressions will be further improved.

Table 2 Correlations of the empirical expressions considering the average of the SQMs with experimental data (takeoff flyovers)

SQMs	R^2	p value	Characteristics of the aircraft
Loudness	0.95	2.62e-8	Wing span, length, cabin width, height, MTOW, fan diameter, takeoff (TO) thrust
Roughness	0.94	5.98e-8	Wing span, length, cabin width, fan diameter, maximum takeoff thrust
Sharpness	0.87	3.07e-6	Wing span, length, cabin width, fan diameter, nacelle length, TO thrust
Tonality	— —	— —	No correlations found

C. Accounting for the Variability of the SQM Within Aircraft Type

The empirical expressions found for the SQMs present a high correlation with the average of the experimental values for each aircraft, as seen in Tables 2 and 3. However, as shown in Figs. 7–10, the SQMs vary within aircraft type because of the operating conditions. The empirical expressions obtained were applied to the entire dataset of flyover measurements, and it was found that the values of R^2 drastically decreased because, without considering the operating conditions of the aircraft, equal values of SQMs were found for the same aircraft type. For instance, the R^2 value of loudness decreased from 0.95 to 0.63 for takeoff and from 0.93 to 0.67 for landing. For roughness, R^2 decreased from 0.94 to 0.42 for takeoff and from 0.90 to 0.30 for landing. This demonstrates the importance of the operating conditions in aircraft annoyance.

New coefficients of the empirical expressions were found by considering the entire dataset of measurements and including the aircraft operating conditions. To the aircraft characteristics providing the best fit for each SQM, described in Tables 2 and 3, were added variables for the aircraft velocity, the altitude, the blade passing frequency, and the rotational speed of the fan. A small number of random measurements were removed from the dataset used to find the coefficients of the empirical expressions of the SQMs in order to use them to test the final expressions.

Some of the aircraft characteristics initially included in Tables 2 and 3 did not contribute to an improved correlation with the experimental data once the operational conditions were included, and therefore were discarded. As expected, the operating conditions with more influence in the results were the altitude of the aircraft and the rotational speed of the fan. Table 4 shows the coefficients of the empirical expression found for the loudness, roughness, and sharpness for takeoff. All the variables considered in the expression are in SI units (International System of Units). The correlations of the

Table 3 Correlations of the empirical expressions considering the average of the SQMs with experimental data (landing flyovers)

SQMs	R^2	p-value	Characteristics of the aircraft
Loudness	0.93	4.22e-8	Wing span, length, cabin width, MLW, BPR, nacelle length, diameter of nose, and main gear tires.
Roughness	0.90	2.63e-7	Wing span, length, cabin width, height, Fan diameter, nacelle length, number of wheels, and diameter of nose and main gear
Sharpness	— —	— —	No correlations found
Tonality	— —	— —	No correlations found

Table 4 Coefficients of the empirical expressions found for the SQMs for takeoff

	Altitude	N_1	Wing span	Height	Length	ϕ fan	Nacelle length	Maximum TO thrust
N_5	−1.40e-1	6.14e-1	— —	5.54	2.17	−2.67e + 1	— —	−1.29e-1
R_5	−1.00e-4	— —	— —	3.80e-3	— —	— —	— —	−8.00e-3
S_5	−9.00e-4	2.40e-3	2.32e-2	— —	3.00e-3	7.37e-1	1.29e-1	−9.3e-3

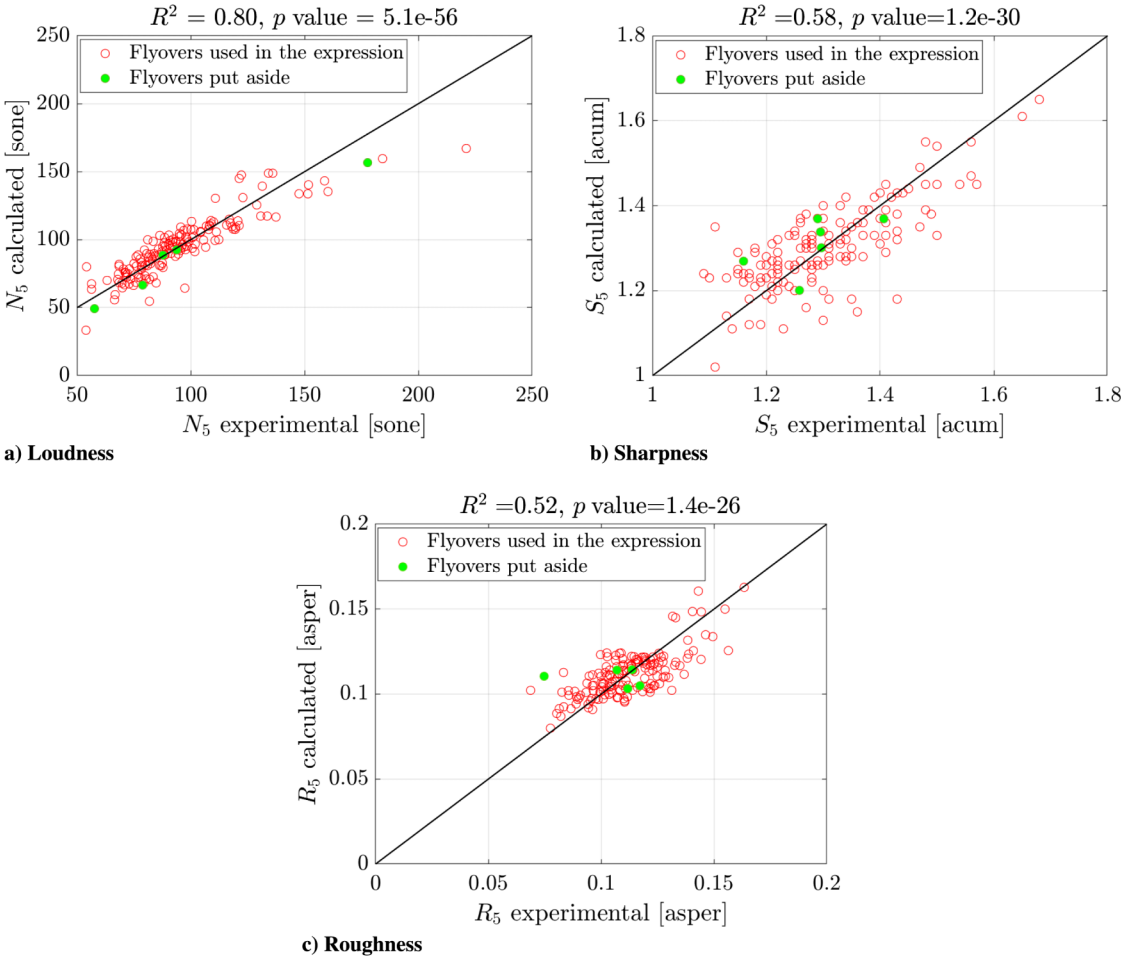

Fig. 13 Comparison of experimental data (x axis) with the results of the empirical expressions (y axis) for takeoff. The black line corresponds to a correlation of $R^2 = 1$.

empirical expressions of the SQMs with the experimental data is shown in Fig. 13. Some measurements were randomly put aside and not used to obtain the expressions in order to test them (green points). A good correlation was obtained for loudness, but sharpness and roughness show weaker results.

The same analysis is now presented for the landing flyovers. Despite the good correlation found for roughness in Tables 2 and 3 with the average experimental data, no empirical expression was able to capture the roughness variation within the same aircraft type. Also, no empirical expression was found for sharpness. Despite the lack of a significant correlation for tonality in Tables 2 and 3, this changed when the operating conditions were introduced, which is not unexpected when considering that the fan is the most relevant source of tonal noise and the sound pressure level of the harmonics depends on the atmospheric propagation effects, and therefore on the altitude. The empirical expression for loudness continues to show a strong correlation with experimental data when considering the entire dataset: similar to what was verified for takeoff.

Table 5 shows the coefficients of the empirical expressions of loudness and tonality for landing aircraft. The two expressions do not have parameters in common; loudness depends only on the dimension of the aircraft, and tonality has a close relation with the

Table 5 Coefficients of the empirical expressions found for the SQMs for landing

	Wing span	Length	Cabin width	Height	Nacelle length	ϕ wheel MLG	— —
N_5	−7.76	6.69e-1	4.82e + 1	1.00e + 1	1.05e + 1	2.94e + 1	— —
	N_1	BPF	Number of fan blades	BPR	ϕ fan	Number of wheels MLG × ϕ	Number of wheels MLG × ϕ
K_5	−3.00e-3	1.00e + 4	3.40e-3	−3.60e-2	2.44e-1	−8.00e-3	−2.20e-2

MLG = main landing gear.

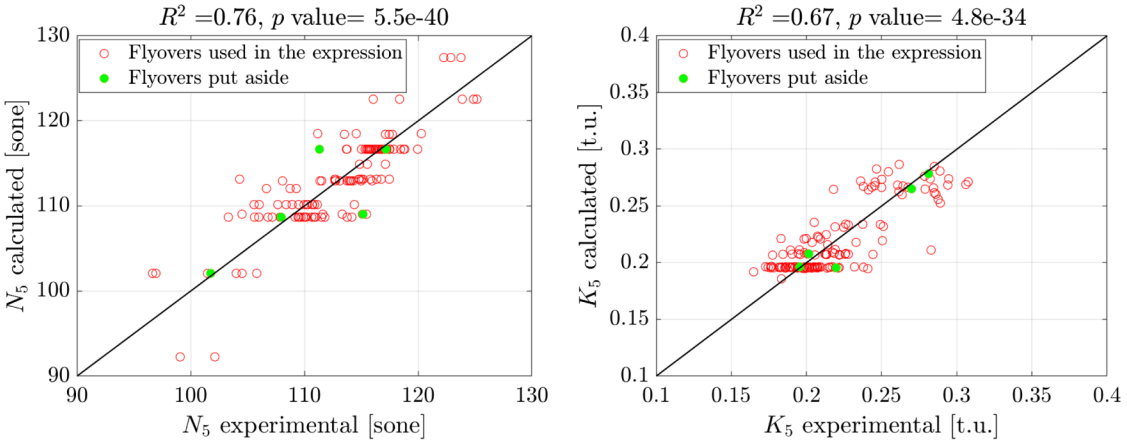

a) Loudness **b) Tonality**

Fig. 14 Comparison of experimental data (x axis) with the results of the empirical expressions (y axis) for landing. The black line corresponds to a correlation of $R^2 = 1$.

operating conditions of the fan, engine parameters, and the landing gear configuration (number of wheels multiplied by their diameter ϕ).

The comparison of the experimental data points with the results obtained using the empirical expressions for landing is shown in Fig. 14. The measurements that were randomly left out the dataset used for finding the coefficients of the empirical expressions show a reasonable agreement with the experimental results (green points).

V. Conclusions

This research uses a large dataset of flyover measurements to investigate the behavior of the sound quality metrics loudness, tonality, sharpness, and roughness during landing and takeoff. The measurement locations were close to the airport, representative of urban areas near airports that are subjected to high levels of annoyance.

It was observed that the values of tonality for the takeoff and landing flyovers were very similar, and the same was verified for roughness. The sharpness values were higher for landing than for takeoff. The aircraft operating conditions and the attenuation of high-frequency noise caused by the propagation on the atmosphere have an important effect on the SQMs. For instance, takeoff trajectories have a high climb rate; therefore, when the aircraft exits the airport limits and enters an urban area, it is already at a high altitude, and high-frequency noise is strongly attenuated by the atmosphere, which results in low values of sharpness.

Although the noise spectrum of takeoff flyovers shows some buzz-saw noise tones, they are not translated into a significant difference in roughness for takeoff and landing. The same is true for tonality during landing; despite the clear peaks of the four first harmonics of the fan, the values of this sound quality metric do not differ greatly for landing and takeoff measurements.

It was shown that the SQMs vary within the same aircraft type because of the aircraft operating conditions. The SQMs can be correlated with design characteristics and operating conditions of the aircraft. Empirical expressions were found for loudness, roughness, and sharpness for takeoff aircraft. Empirical expressions for loudness and tonality were obtained for landing aircraft. These expressions showed a reasonable correlation with the experimental data when considering the limited information available, since only the velocity and altitude of the aircraft and the rotational speed and blade passing frequency of the fan could be estimated.

The obtained empirical expressions provide important information about the characteristics of the aircraft that can contribute to a sharper or a more tonal sound, and they indicate that the SQMs can be taken into account in the design phase of an aircraft. However, more experimental data are required to further improve and validate these empirical expressions for other locations around the airport.

References

[1] Basner, M., and McGuire, S., "WHO Environmental Noise Guidelines for the European Region: A Systematic Review on Environmental Noise and Effects on Sleep," *International Journal of Environmental Research and Public Health*, Vol. 15, No. 3, 2018, Paper 519. https://doi.org/10.3390/ijerph15030519

[2] Scharf, B., and Hellman, R., "Comparison of Various Methods for Predicting the Loudness and Acceptability of Noise, Part II," U.S. Environmental Protection Agency TR 550/9-79-102, 1977.

[3] Lopes, L. V., Iyer, V. R., and Born, J. C., "Robust Acoustic Objective Functions and Sensitivities in Adjoint-Based Design Optimizations," *AIAA Journal*, Vol. 57, No. 8, 2019, pp. 3185–3199. https://doi.org/10.2514/1.J056518

[4] Antoine, N., and Kroo, I., "Framework for Aircraft Conceptual Design and Environmental Performance Studies," *AIAA Journal*, Vol. 43, No. 10, 2005, pp. 2100–2109. https://doi.org/10.2514/1.13017

[5] More, S. R., "Aircraft Noise Characteristics and Metrics," Ph.D. Dissertation, Purdue Univ., West Lafayette, IN, 2010.

[6] Sahai, A. K., Snellen, M., Simos, D. G., and Stumpf, E., "Aircraft Design Optimization for Lowering Community Noise Exposure Based on Annoyance Metrics," *Journal of Aircraft*, Vol. 54, No. 6, 2017, pp. 2257–2269. https://doi.org/10.2514/1.C034009

[7] Sahai, A. K., van Hermelen, T., and Simons, D. G., "Methodology for Designing Aircraft Having Optimal Sound Signatures," *Journal of the Acoustical Society of America*, Vol. 141, No. 5, 2017, pp. 3688–3688. https://doi.org/10.1121/1.4988028

[8] Antoine, N., and Kroo, I., "Aircraft Optimization for Minimal Environmental Impact," *Journal of Aircraft*, Vol. 41, No. 4, 2004, pp. 790–797. https://doi.org/10.2514/1.71

[9] Ho-Huu, V., Hartjes, S., Visser, H., and Curran, R., "Integrated Design and Allocation of Optimal Aircraft Departure Routes," *Transportation Research Part D: Transport and Environment*, Vol. 63, Aug. 2018, pp. 689–705. https://doi.org/10.1016/j.trd.2018.07.006

[10] Vieira, A., Mehmood, U., Merino-Martínez, R., Snellen, M., and Simon, D., "Variability of Sound Quality Metrics for Different Aircraft Types During Landing and Take-Off," *25th AIAA/CEAS Aeroacoustics Conference*, AIAA Paper 2019-2512, May 2019. https://doi.org/10.2514/6.2019-2512

[11] "Acoustics–Methods for Calculating Loudness–Part 1: Zwicker Method," International Organization for Standardization STD ISO 532-1: 2017, 2017.

[12] Zwicker, E., Fastl, H., Widmann, U., Kurakata, K., Kuwano, S., and Namba, S., "Program for Calculating Loudness According to Din 45631 (ISO 532b)," *Journal of the Acoustical Society of Japan*, Vol. 12, No. 1, 1991, pp. 39–42. https://doi.org/10.1250/ast.12.39

[13] Terhardt, E., "Calculating Virtual Pitch," *Hearing Research*, Vol. 1, No. 2, 1979, pp. 155–182. https://doi.org/10.1016/0378-5955(79)90025-X

[14] Allen, J. B., "Harvey Fletcher's Role in the Creation of Communication Acoustics," *Journal of the Acoustical Society of America*, Vol. 99, No. 4, 1996, pp. 1825–1839. https://doi.org/10.1121/1.415364

[15] von Bismarck, G., "Sharpness as an Attribute of the Timbre of Steady Sounds," *Acta Acustica United with Acustica*, Vol. 30, No. 3, 1974, pp. 159–172.

[16] Aures, W., "Procedure for Calculating the Sensory Euphony of Arbitrary Sound Signals," *Acustica*, Vol. 59, No. 2, 1985, pp. 130–141.

[17] Terhardt, E., Stoll, G., and Seewann, M., "Algorithm for Extraction of Pitch and Pitch Salience from Complex Tonal Signals," *Journal of the Acoustical Society of America*, Vol. 71, No. 3, 1982, pp. 679–688. https://doi.org/10.1121/1.387544

[18] Zwicker, E., and Fastl, H., *Psychoacoustics: Facts and Models*, 3rd ed., No. 22 in Springer Series in Information Sciences, Springer, Berlin, 2007.

[19] Aures, W., "A Procedure for Calculating Auditory Roughness," *Acustica*, Vol. 58, 1985, pp. 268–281.

[20] Daniel, P., and Weber, R., "Psychoacoustical Roughness: Implementation of an Optimized Model," *Acta Acustica United with Acustica*, Vol. 83, No. 1, 1997, pp. 113–123.

[21] Underbrink, J. R., "Circularly Symmetric, Zero Redundancy, Planar Array Having Broad Frequency Range Applications," U.S. Patent 6,205,224 B1, 2001.

[22] Merino-Martinez, R., Snellen, M., and Simons, D. G., "Functional Beamforming Applied to Imaging of Flyover Noise on Landing Aircraft," *Journal of Aircraft*, Vol. 53, No. 6, 2016, pp. 1830–1843. https://doi.org/10.2514/1.C033691

[23] Redonnet, S., Desquesnes, G., Manoha, E., and Parzani, C., "Numerical Study of Acoustic Installation Effects with a Computational Aeroacoustics Method," *AIAA Journal*, Vol. 48, No. 5, 2010, pp. 929–937. https://doi.org/10.2514/1.42153

[24] Vieira, A., Snellen, M., and Simons, D., "Assessing the Shielding of Engine Noise by the Wings for Current Aircraft Using Model Predictions and Measurements," *Journal of the Acoustical Society of America*, Vol. 143, No. 1, 2018, pp. 388–398. https://doi.org/10.1121/1.5020798

[25] Bulté, J., and Redonnet, S., "Landing Gear Noise Identification Using Phased Array with Experimental and Computational Data," *AIAA Journal*, Vol. 55, No. 11, 2017, pp. 3839–3850. https://doi.org/10.2514/1.J055643

[26] Guo, Y. P., and Joshi, M., "Noise Characteristics of Aircraft High Lift Systems," *AIAA Journal*, Vol. 41, No. 7, 2003, pp. 1247–1256. https://doi.org/10.2514/2.2093

[27] Adetifa, O., McAlpine, A., and Gabard, G., "Nonlinear Propagation of Supersonic Fan Tones in Turbofan Intake Ducts," *AIAA Journal*, Vol. 56, No. 1, 2018, pp. 316–328. https://doi.org/10.2514/1.J056121

[28] Wilkinson, M., and Joseph, P., "Comparison of Strategies for the Active Control of Buzz-Saw Tones," *AIAA Journal*, Vol. 44, No. 6, 2006, pp. 1150–1157. https://doi.org/10.2514/1.16175

C. Pettit
Associate Editor